The 24th International Conference on Computer Animation and Social Agents

Multi-layer Structural Wound Synthesis on 3D Face

Chung-Yeon Lee, Sangyong Lee, and Seongah Chin
Visual and & Virtual Computing Laboratory
Division of Multimedia Engineering
Sungkyul University

Outline

- Introduction
  - Motivation
  - Skin layers and facial-tissue depth
  - Related works
- Methodology
  - Facial Tissue Depth Map
  - Wound Depth Map
  - Model Coordination Mapping
- Experimental results
  - Validation of Wound Depths
  - Validation of Various Wound Depths at Different Locations of the Face
- Conclusion
  - Summary
  - Future works

Introduction

- Motivation
  - Reconstructing 3D faces based on the anatomical structure of the face
  - Realistic wound synthesis on 3D face
  - An automatic method of wound synthesis on 3D face is needed

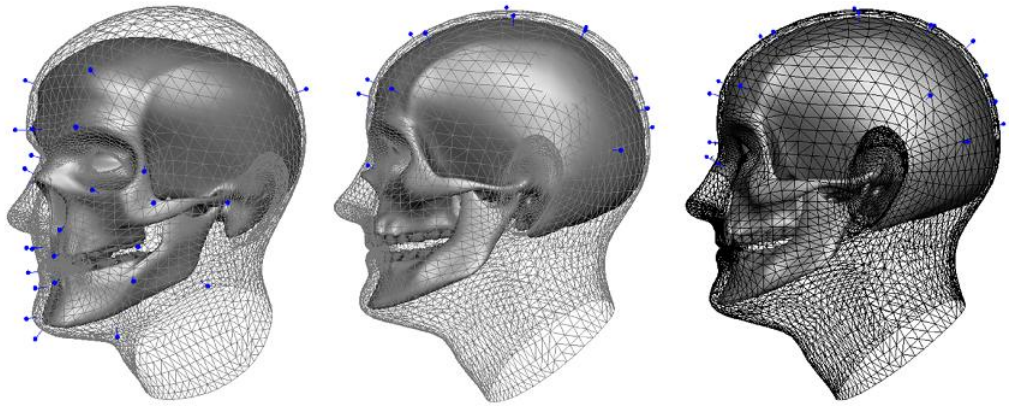

* Olusola O. Aina, 2009.

Introduction

- Skin layers
  - Skin is composed of three primary layers: *The epidermis, The dermis, The subcutis*

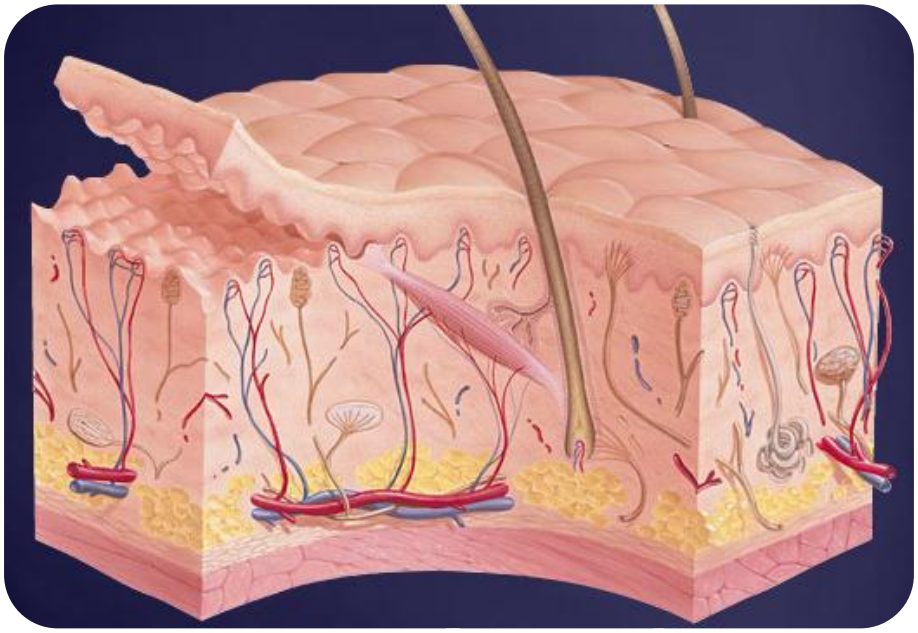

* Source from National Geographic

Introduction

- Skin layers
  - Skin is composed of three primary layers: *The epidermis, The dermis, The subcutis*

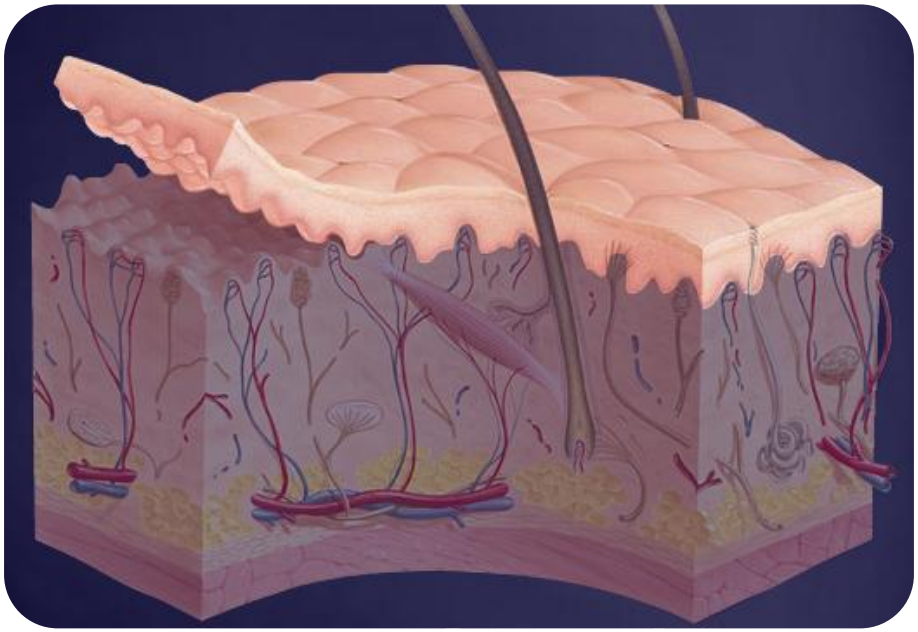

* Source from National Geographic

Introduction

- Skin layers
  - Skin is composed of three primary layers: *The epidermis, The dermis, The subcutis*

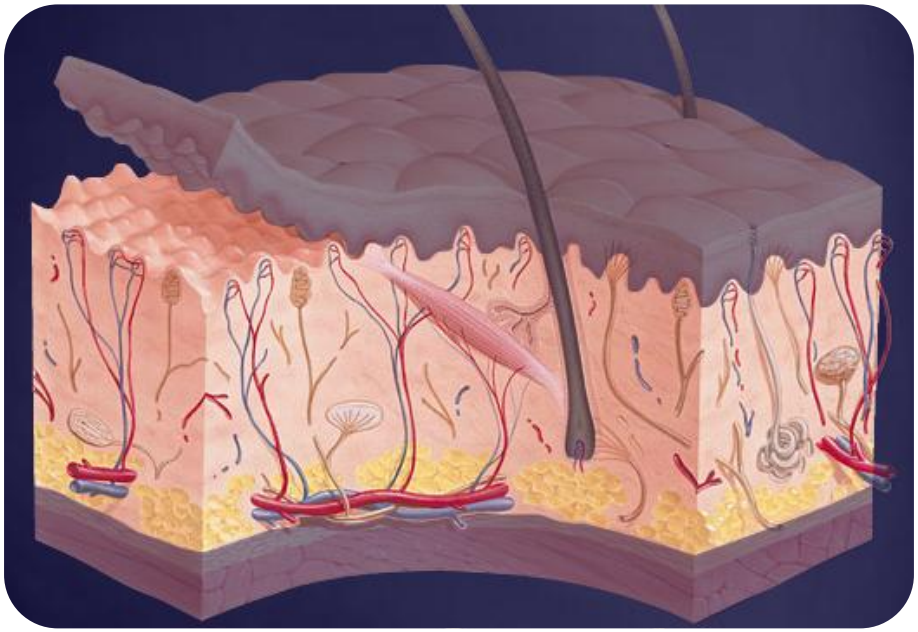

* Source from National Geographic

Introduction

- Skin layers
  - Skin is composed of three primary layers: *The epidermis, The dermis, The subcutis*

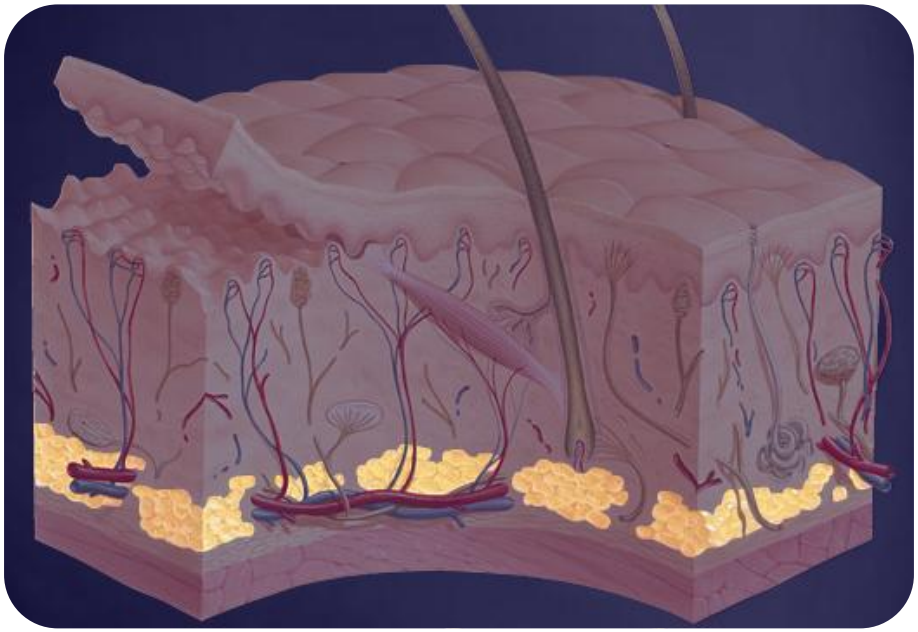

* Source from National Geographic

Introduction

- Facial tissue depth
  - The depth of facial tissue is dependent on the location of the skin on the face.
  - Facial Tissue Depth Map (FTDM) needs to be modeled taking into account of tissue layers including epidermis, dermis, and subcutis.

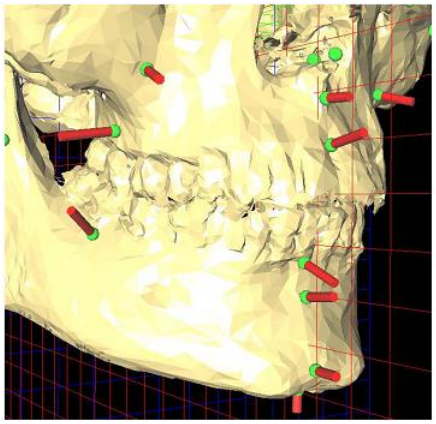

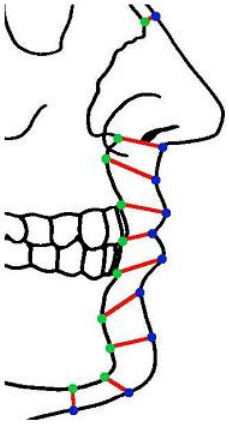

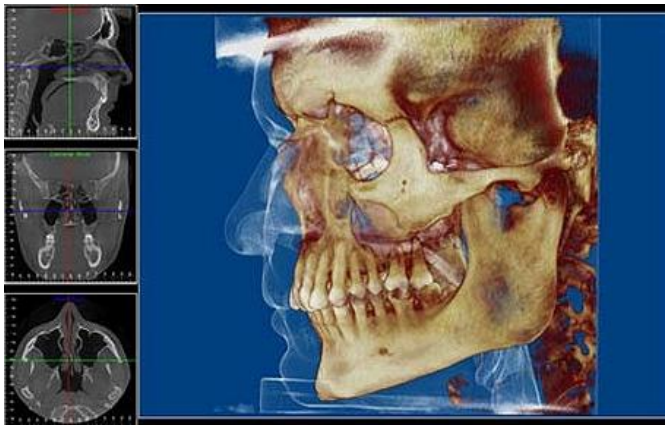

Introduction

- Facial tissue depth
  - The Tallied-Facial-Soft-Tissue-Depth-Data (produced by Stephan and Simpson)
    - Stephan and Simpson, “Facial soft tissue depths in craniofacial identification,” *Journal of Forensic Sciences.*, 53(6), 2008

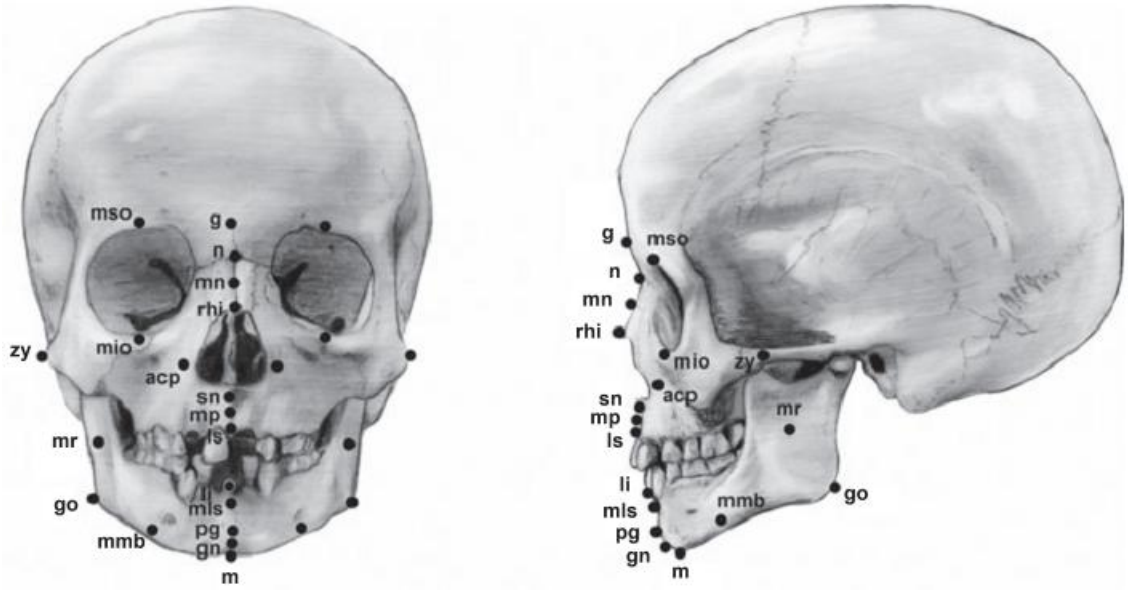

Introduction

2011 Tallied-Facial-Soft-Tissue-Depth-Data: ADULTS (≥18 years)

Soft Tissue Depth Measurement	Total Weighted Mean	*n*	No. of Samples	Weighted Mean for *s* Studies	*s*	*n*	No. of Samples	Estimated Minimum (Mean - 3 z-scores)	Estimated Maximum (Mean +3 z-scores)
Median points									
op-op'	6.5	1452	54	7.0	2.0	1171	36	1.5	12.5
v-v'	5.0	1402	46	4.5	1.0	1132	32	1.0	8.0
g-g'	5.5	6342	173	5.5	1.0	5005	122	2.5	8.5
n-n'	6.5	6786	169	6.0	1.5	5072	114	1.0	10.5
mn-mn'	4.0	1272	67	4.0	1.0	918	37	0.5	10.5
rhi-rhi'	3.0	6022	153	3.0	1.0	4848	105	0.0	6.0
sn-sn'	13.0	1823	80	13.0	3.0	1225	45	4.0	21.5
mp-mp'	11.5	6094	127	11.0	2.5	4501	83	3.5	18.5
ls-ls'	11.5	5491	138	11.5	3.0	4561	100	3.0	19.5
li-li'	13.0	5271	115	13.0	2.5	4362	80	5.0	21.0
mls-mls'	11.0	6396	170	11.0	2.0	5132	117	5.5	16.5
pg-pg'	11.0	7382	179	11.0	2.5	5518	115	3.5	18.5
gn-gn'	8.5	545	18	8.5	3.0	381	10	-1.0	18.0
m-m'	7.0	5088	153	7.0	2.0	4249	110	0.5	13.5
Bilateral points									
mso-mso'	6.0	2795	89	6.0	1.5	2366	56	1.5	10.5
mio-mio'	6.5	2866	100	7.0	3.5	2438	68	-3.5	17.5
acp-acp'	9.5	1558	44	9.5	2.5	1408	32	2.5	16.5
go-go'	10.5	4746	123	10.5	6.0	3858	85	-7.5	28.5
zy-zy'	6.5	4660	112	6.0	2.5	3550	69	-1.0	13.0
sC-sC'	9.5	3289	52	9.5	2.0	3264	50	3.5	16.0
iC-iC'	10.5	1335	29	10.5	2.0	1308	27	4.5	16.5
sM^2-$sM^{2'}$	24.0	1943	48	24.5	5.5	1710	38	8.5	41.0
iM_2-iM_2'	18.5	1535	43	19.0	5.0	1302	33	4.0	33.5
mr-mr'	17.5	3009	62	17.5	4.0	2788	39	5.5	30.0
mmb-mmb'	10.5	1086	28	10.5	4.5	699	23	-2.5	23.5

- C. Stephan, CRANIOFACIALidentification.com
- *www.craniofacialidentification.com/2011_T-table_ADULTdataONLY.pdf*

Introduction

- Jeffrey Berkley et al., 2004.
  - Analysis on suturing processing of surgical operations.
  - Simulated in computational model using finite element model.

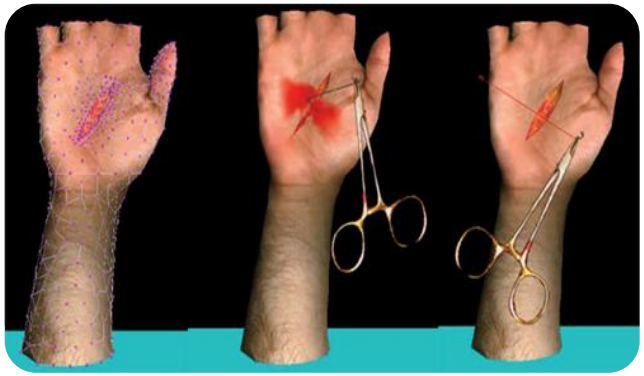

- Yuzhong Shen et al., 2006.
  - A virtual treatment training system for removal of debridement on wounds.

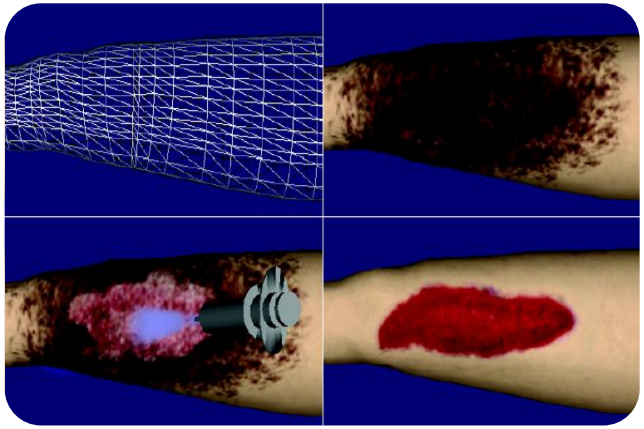

Introduction

- Peter Oppenheimer et al., 2002.
  - Compositing local surface features of cutaneous wounds onto 2d / 3d patient models.
  - The wound database is generated from clinically captured photographic images.
  - Extracted wound images using Adobe Photoshop and attached the images onto 3d patient model made by using a 3d authoring software (3DMeNow).

Methodology

- Schematic approaches

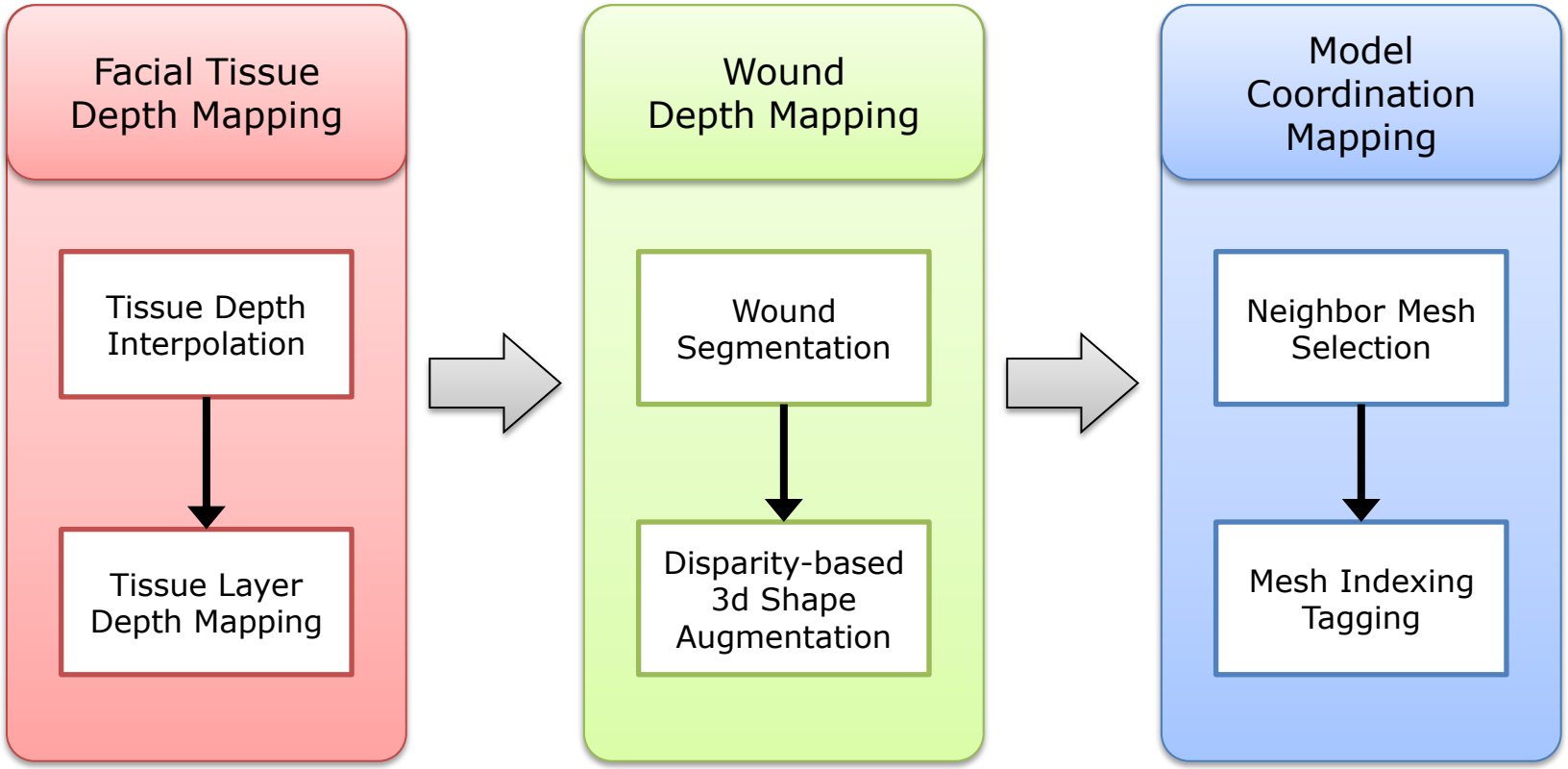

Facial Tissue Depth Map

- Tissue depth interpolation
  - The measured facial tissue depth values are interpolated by using Thin-plate spline (TPS)

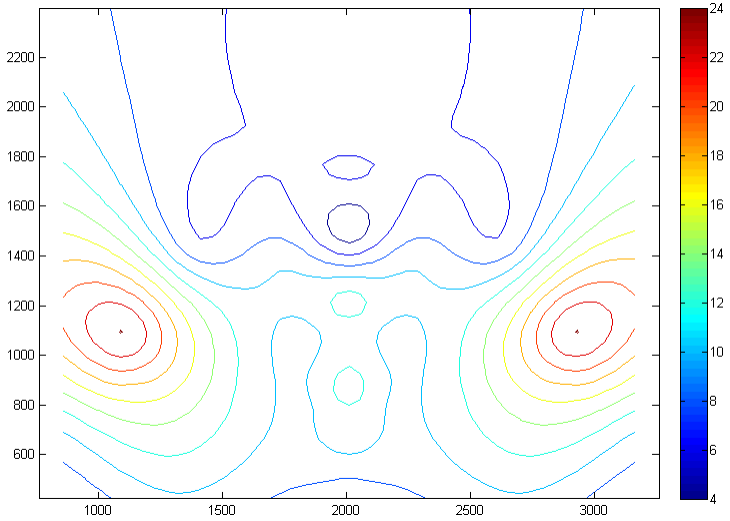

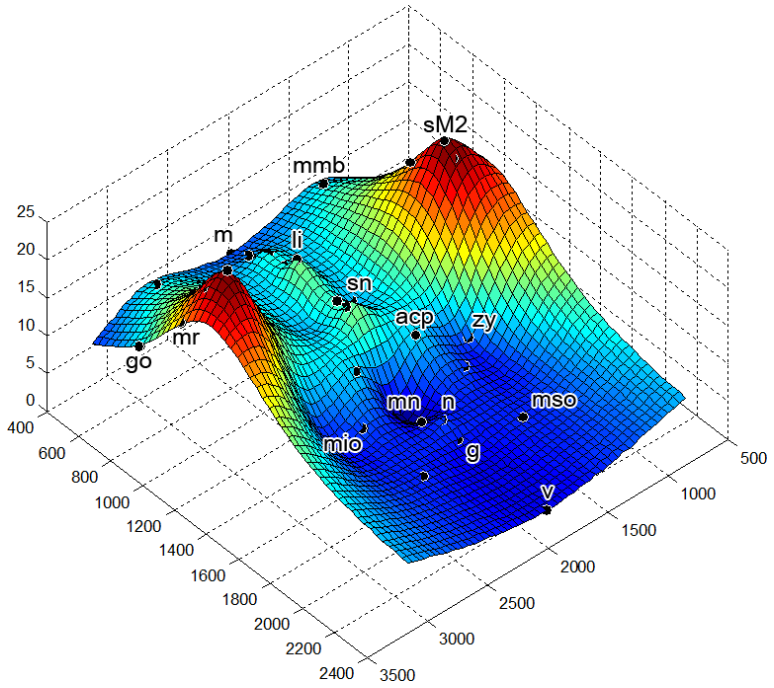

$$FTDM\left[f(x,y) \right] = \iint_{R^2} \left(f_{xx}^2 + 2 f_{xy}^2 + f_{yy}^2 \right) dxdy$$

Facial Tissue Depth Map

- Tissue layer depth mapping on the 3d face model
  - A set of points on the FTDM of an entire face are represented in the 3D face model.
  - Results of FTDM on 7,343 vertices of 3d face model in *mm* sized depth values.

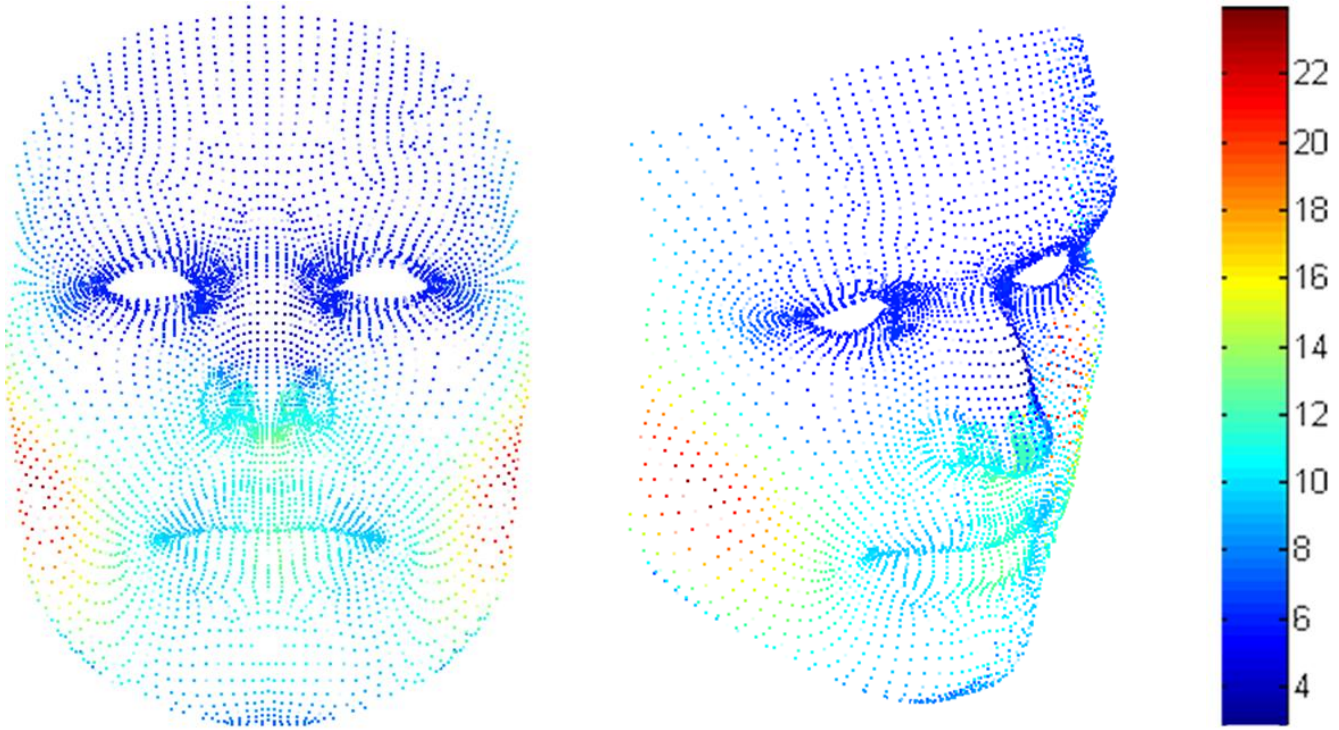

Wound Depth Map

- Wound Texture Images
  - Various wound images are collected and classified into types of wounds.
  - It consists of diverse wound images including abrasion, stab, burn, incision, and so on.
  - We filtered the images, extracting only the wound areas from the surrounding skin.
  - However, the sample images do not have 3D geometry.

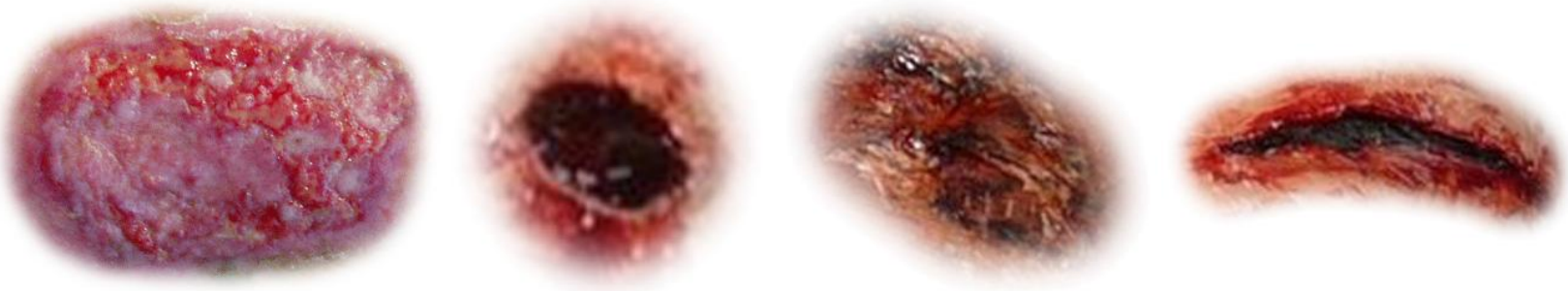

abrasion stab burn incision

Wound Depth Map

- Tissue layer segmentation
  - Hue-based tissue layer segmentation has been developed to build a volumetric geometry model for a wound.

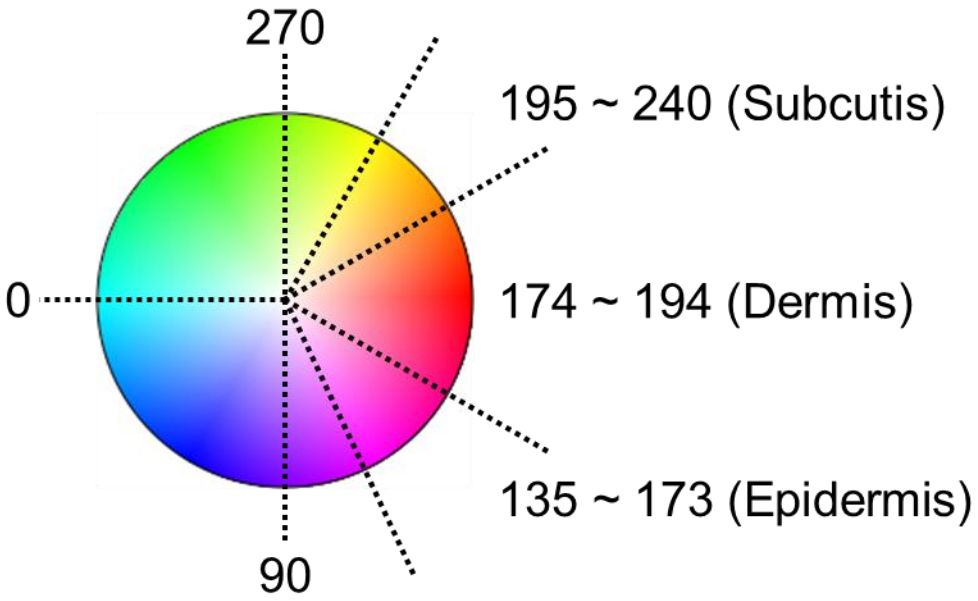

Wound Depth Map

- Tissue layer segmentation
  - Segmentation is region-based, not pixel-based, using 16 partitions of a wound.
  - The dominant tissue layer is determined by comparing sum of pixels in each layer.

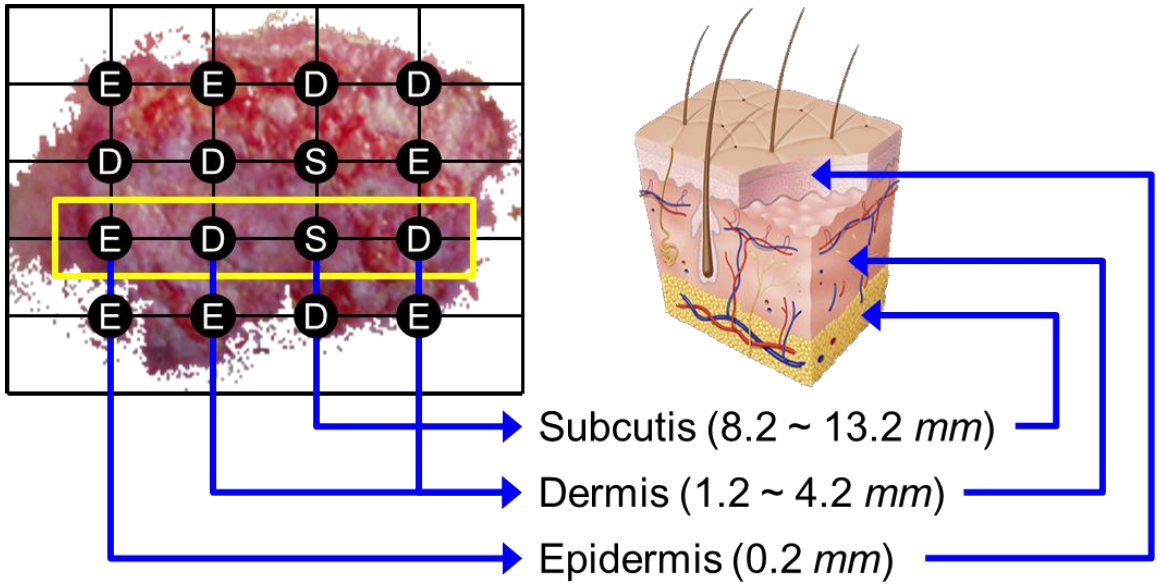

Wound Depth Map

- Disparity-based 3d shape augmentation
  - Disparity parameters caused by the interpupillary distance (IPD) are applied to the segmented wound geometry model to implement the disparity due to the curved surface on the face and realise the volumetric geometry for a realistic 3d wound shape.
  - Normalised mean of the hue value $NH_{i,j}$ is used to gauge the disparity parameter $\delta_{i,j}$ for every partition computed.

$$\delta_{i,j} = \left(\frac{IPD * NH_{i,j}}{2} \right) * \frac{z}{w*(z+d)}$$

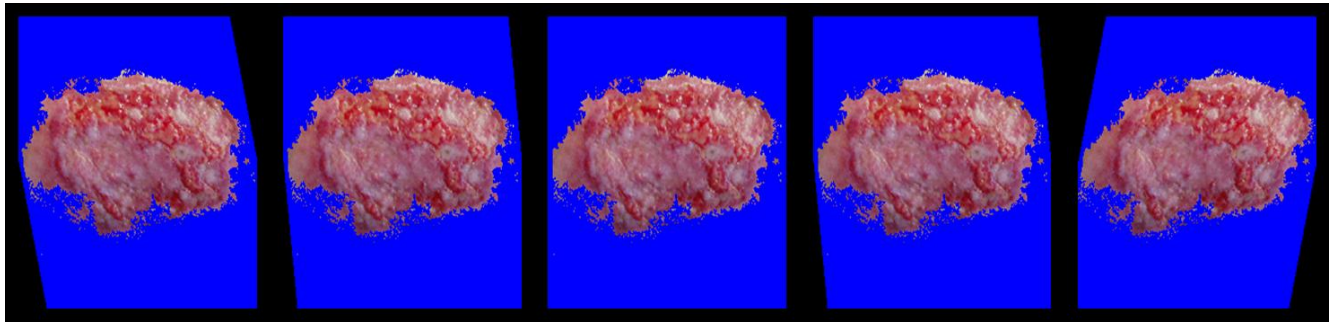

Model Coordination Mapping

- Wound Positioning
  - $P' = (NV)^{-1} P$
    - P': 3d coordinate, P: 2d coordinate
    - N: perspective projection matrix
    - V: viewport transformation matrix

$$N = \begin{bmatrix} \frac{2n}{r-1} & 0 & \frac{r+1}{r-1} & 0 \\ 0 & \frac{2n}{t-b} & \frac{t+b}{t-b} & 0 \\ 0 & 0 & -\frac{f+n}{f-n} & -\frac{2fn}{f-n} \\ 0 & 0 & -1 & 0 \end{bmatrix} \quad V = \begin{bmatrix} \frac{w}{2} & 0 & 0 & l+\frac{w}{2} \\ 0 & \frac{h}{2} & 0 & b+\frac{h}{2} \\ 0 & 0 & 0 & 1 \\ 0 & 0 & 0 & 1 \end{bmatrix}$$

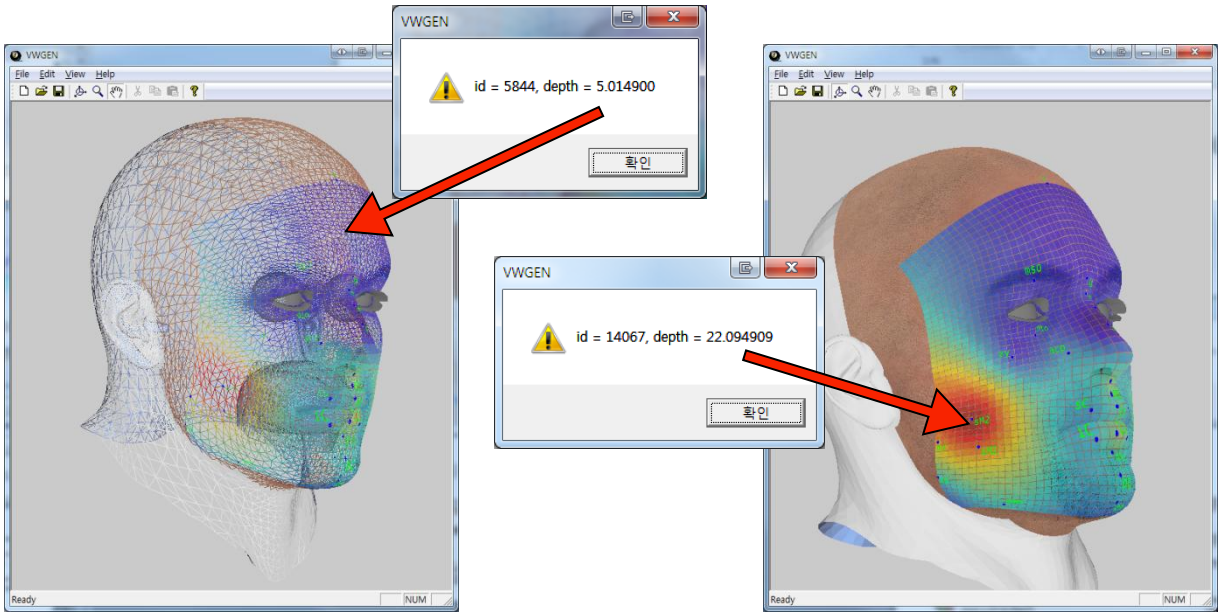

Model Coordination Mapping

- Neighboring meshes selection
  - The area on which we will implement the wound on the 3D face model is composed of 36 vertices and 50 triangular meshes, which the user can select when wishing to add a wound.
  - All meshes need to be tagged with consecutive indices for wound depth mapping and wound texture mapping.

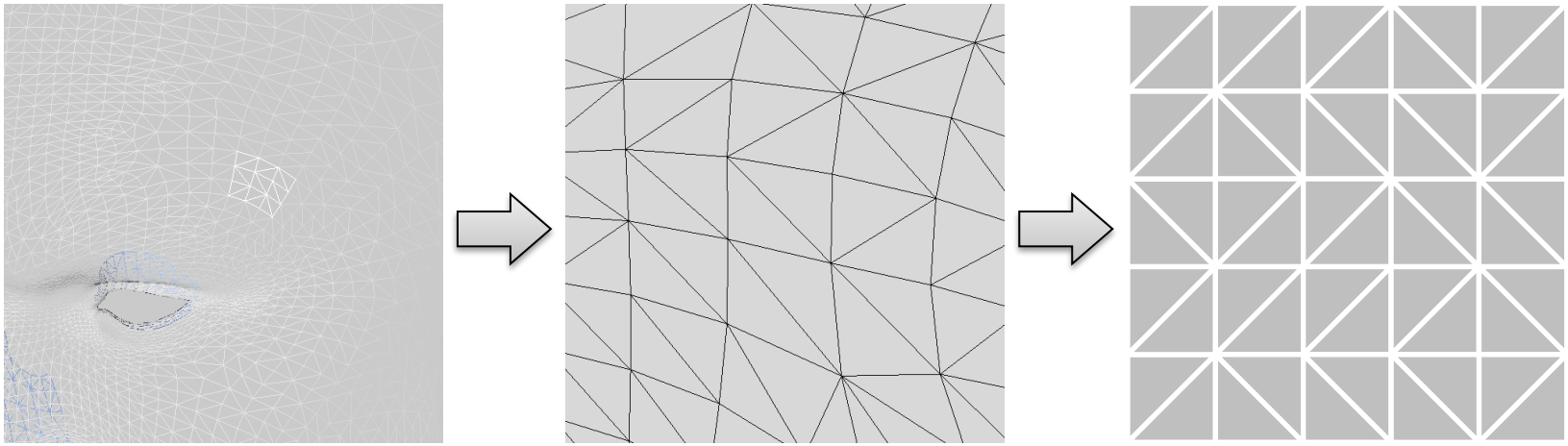

Model Coordination Mapping

- Neighboring meshes selection
  - First, we find f_q, the opposite mesh to the mesh chosen by the user, f_p, and create mesh lists fl_{tvs} and fl_{ovs}
    - fl_{tvs} : a mesh list composed of meshes that have two vertices that are identical to two of the four v ertices, f_p and f_q
    - fl_{ovs} : a mesh list composed of meshes that have only one vertex that is identical to one of f_p and f_q

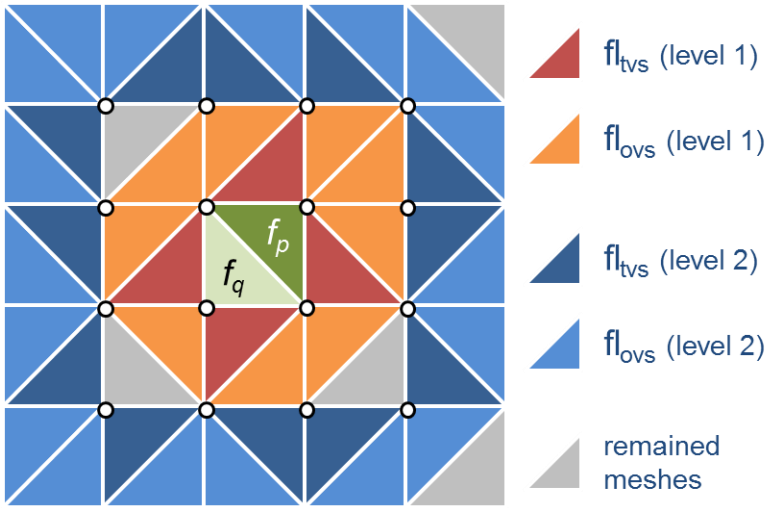

Model Coordination Mapping

- Neighboring meshes selection
  - After that, we create a first level for mesh list fl_{n1} that combines fl_{tvs}, fl_{ovs}, and some remaining meshes, which are opposite meshes of one of fl_{tvs} or fl_{ovs}
  - Using the same rules, we create fl_{n2} for the second level of neighbouring meshes.

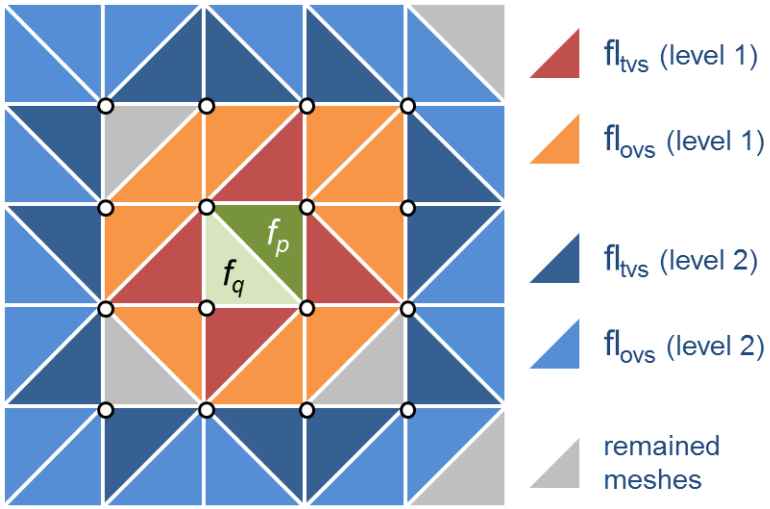

Model Coordination Mapping

- Neighboring meshes selection

Model Coordination Mapping

- Mesh index tagging
  - The meshes for the entire wound area are tagged with consecutive indices from a corner mesh to a centre mesh in a counter-clockwise order.
  - Because there are two types of mesh direction, the first mesh, f_n and the turning flag, z needs to be determined according to the following method.

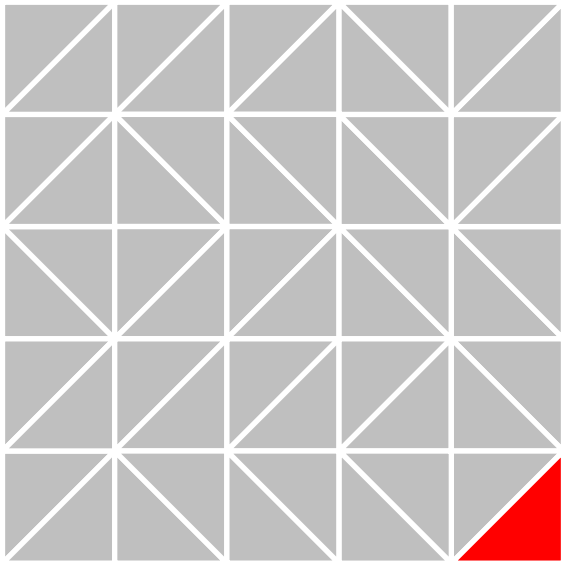

Model Coordination Mapping

- Mesh index tagging
  - The meshes for the entire wound area are tagged with consecutive indices from a corner mesh to a centre mesh in a counter-clockwise order.
  - Because there are two types of mesh direction, the first mesh, f_n and the turning flag, z needs to be determined according to the following method.
    - $v_{nb} \in fl_{ovs}$ && $v_{nb} = v_{pa}$, then $f_n \leftarrow f_2$, $z \leftarrow 0$
    - $v_{nb} \in fl_{ovs}$ && $v_{nb} \neq v_{pa}$ && $v_{nb} = v_{na} = v_{mc}$, then $f_n \leftarrow f_1$, $z \leftarrow 1$

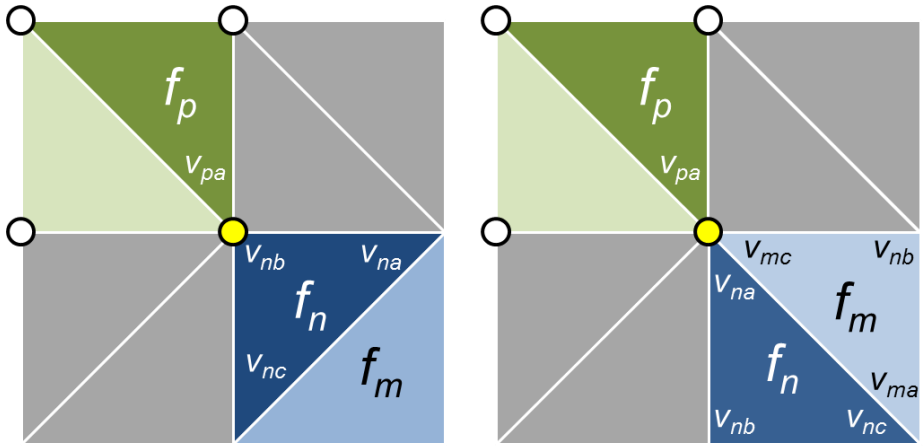

(a) $v_{nb} = v_{pa}$ (b) $v_{nb} \neq v_{pa}$

Model Coordination Mapping

- Mesh index tagging
  - (2) Switching of the turning flag *z*:
    - z ← 0, if f_{xa} and f_{xb} are identical to the two of f_n (v_{na}, v_{nb} *or* v_{nb}, v_{nc})
    - $z \leftarrow 1$, if f_{xb} and f_{xc} are identical to the two of f_n (v_{na}, v_{nb} *or* v_{nb}, v_{nc})
  - (3) A mesh f_y, which is the opposite mesh of f_x, becomes f_{k+1}, and then increment *k*.

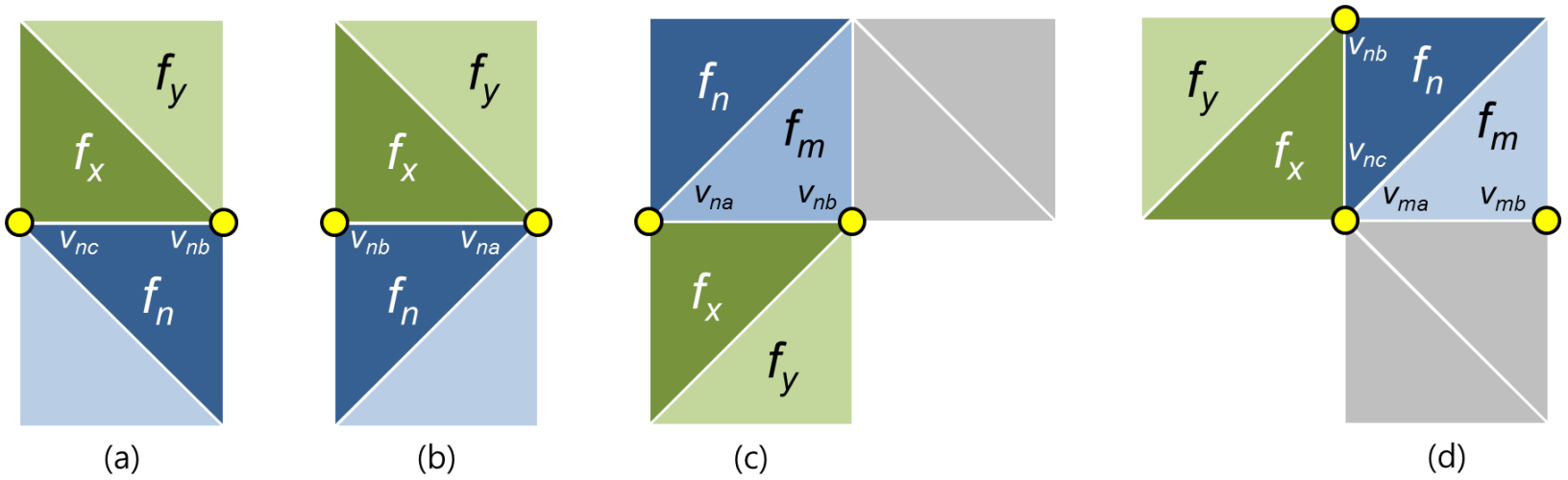

Model Coordination Mapping

- Mesh index tagging
  - ※ If not all neighbouring meshes are satisfied after step (1):
    - i) If the next mesh is located on the left side, and not on the forward side (Fig. d):
      - The next mesh can be found by switching the turning flag z and searching again.
    - ii) If the next mesh, f_x, does not adhere to f_n, as shown in (Fig. c):
      - The next mesh has two vertices identical to v_{ma} and v_{mb} of f_m.

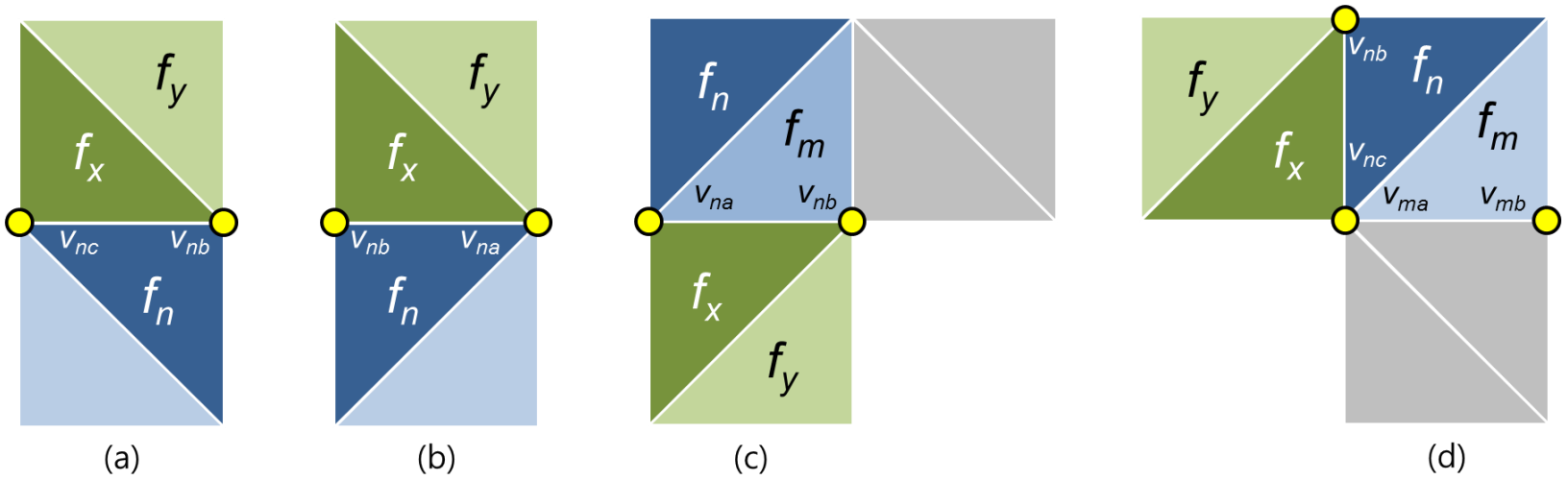

Model Coordination Mapping

- Mesh index tagging

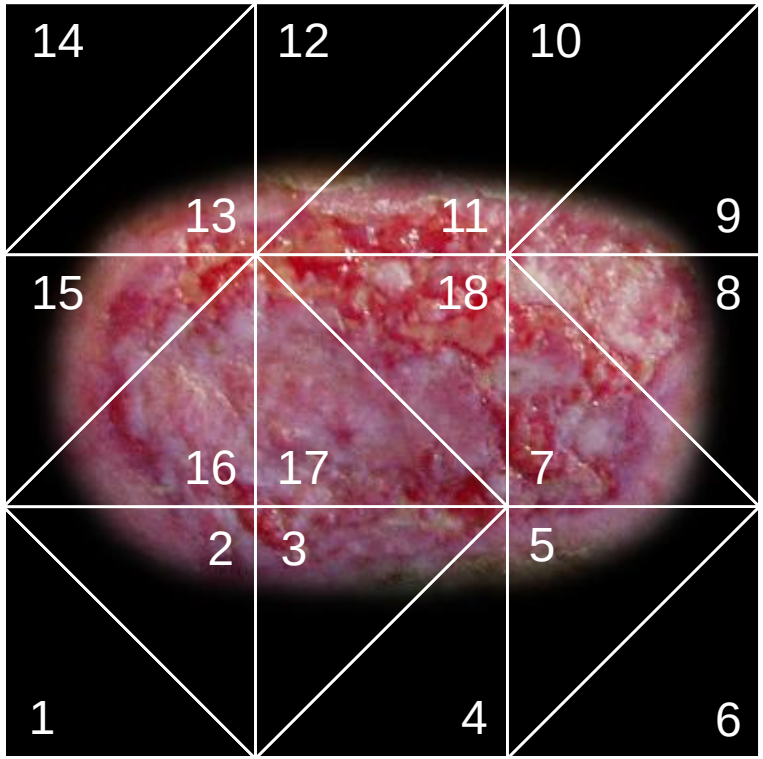

Experimental Results

- Validation of Wound Depths

Experimental Results

- Validation of Wound Depths

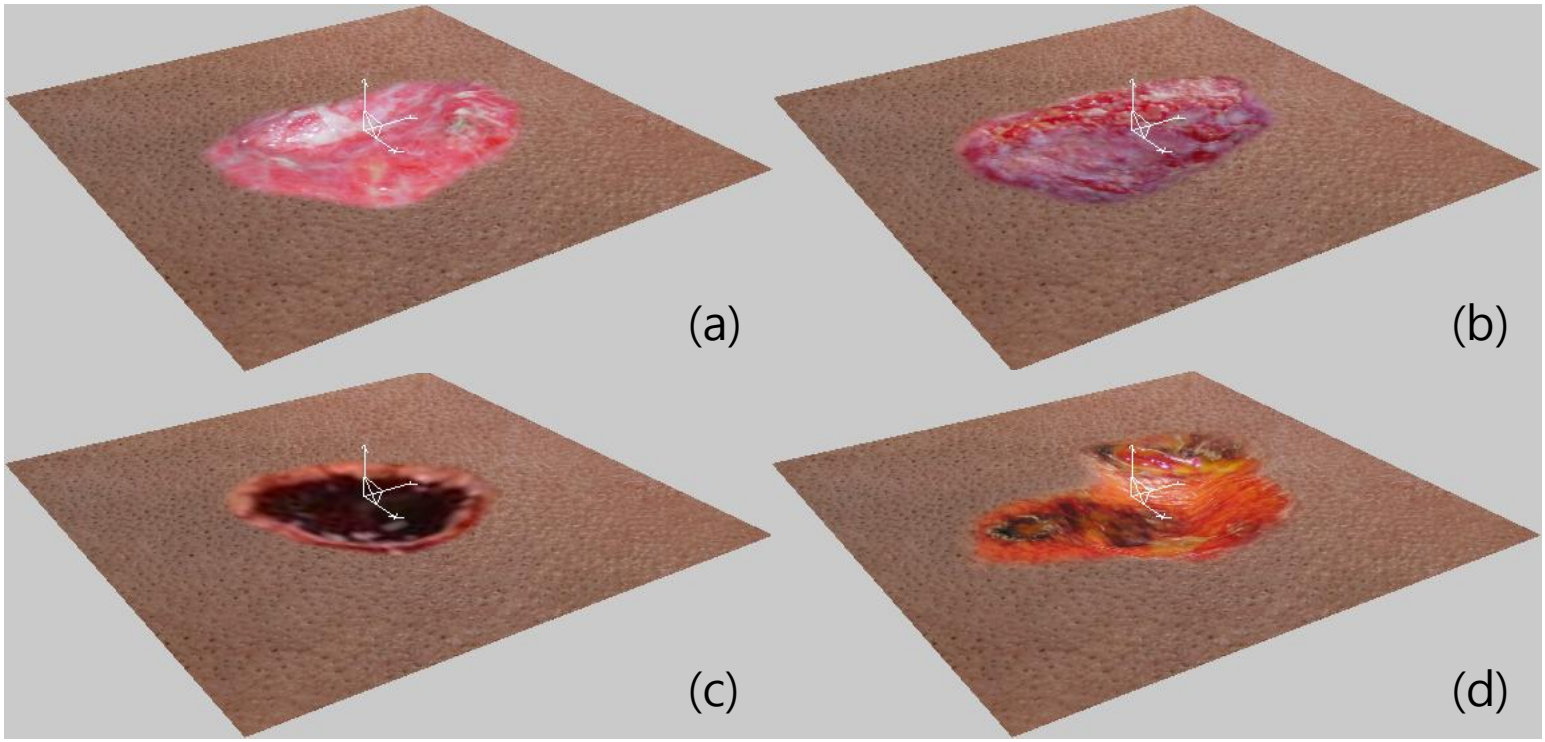

Experimental Results

- Validation of Wound Depths

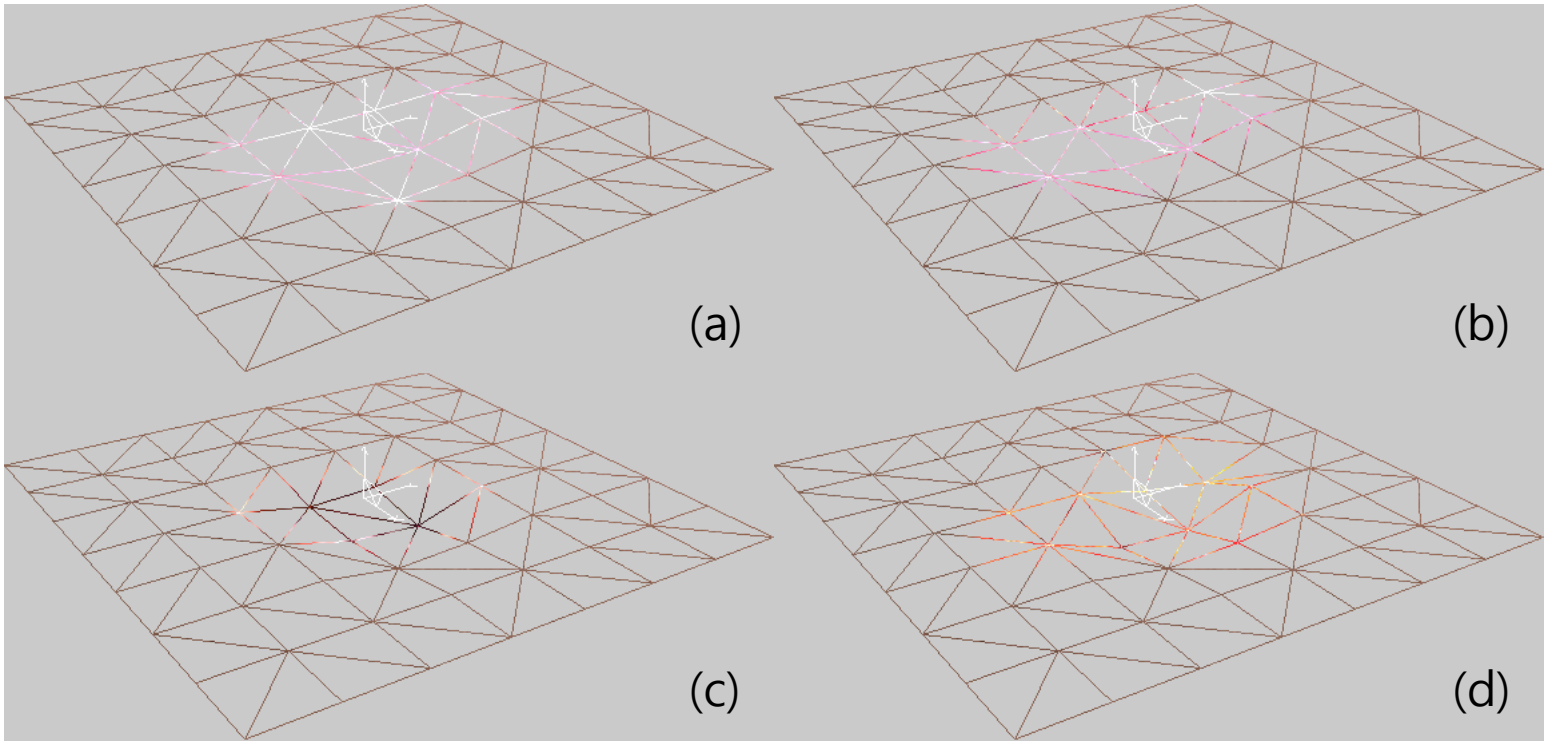

Experimental Results

- 3D facial wound synthesis system
  - A realistic 3d human face was made by using an 3d authoring tool and was converted into an ASCII formatted data for comprehensive manipulations.
  - The model is composed of 13,680 polygons and 17,762 vertices. (Face only: 7344 / 14432)
  - The resolution of texture image is 4,000 square pixels.
  - To simulate wound synthesis on the face model, we developed a 3d facial wound synthesis system using OpenGL and MFC.

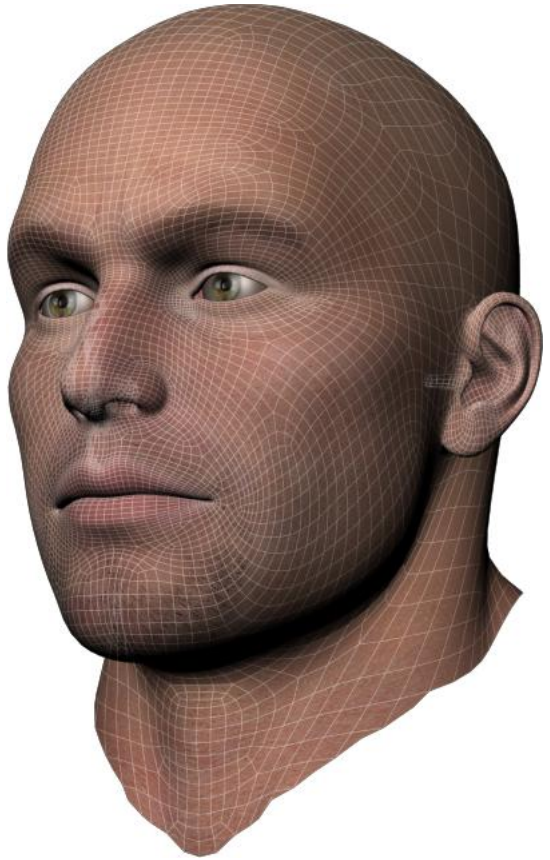

Experimental Results

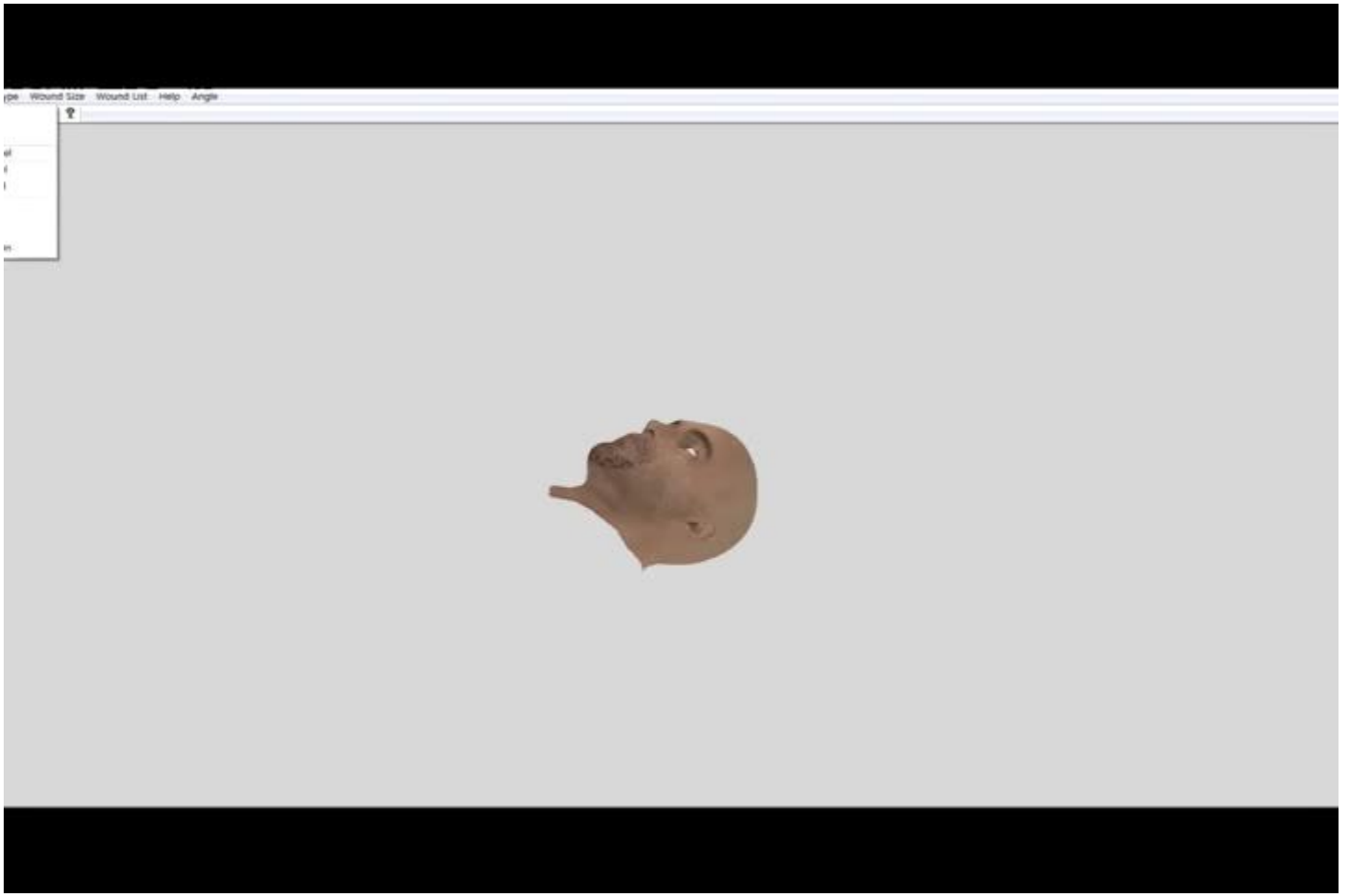

Experimental Results

- Validation of different locations of the face

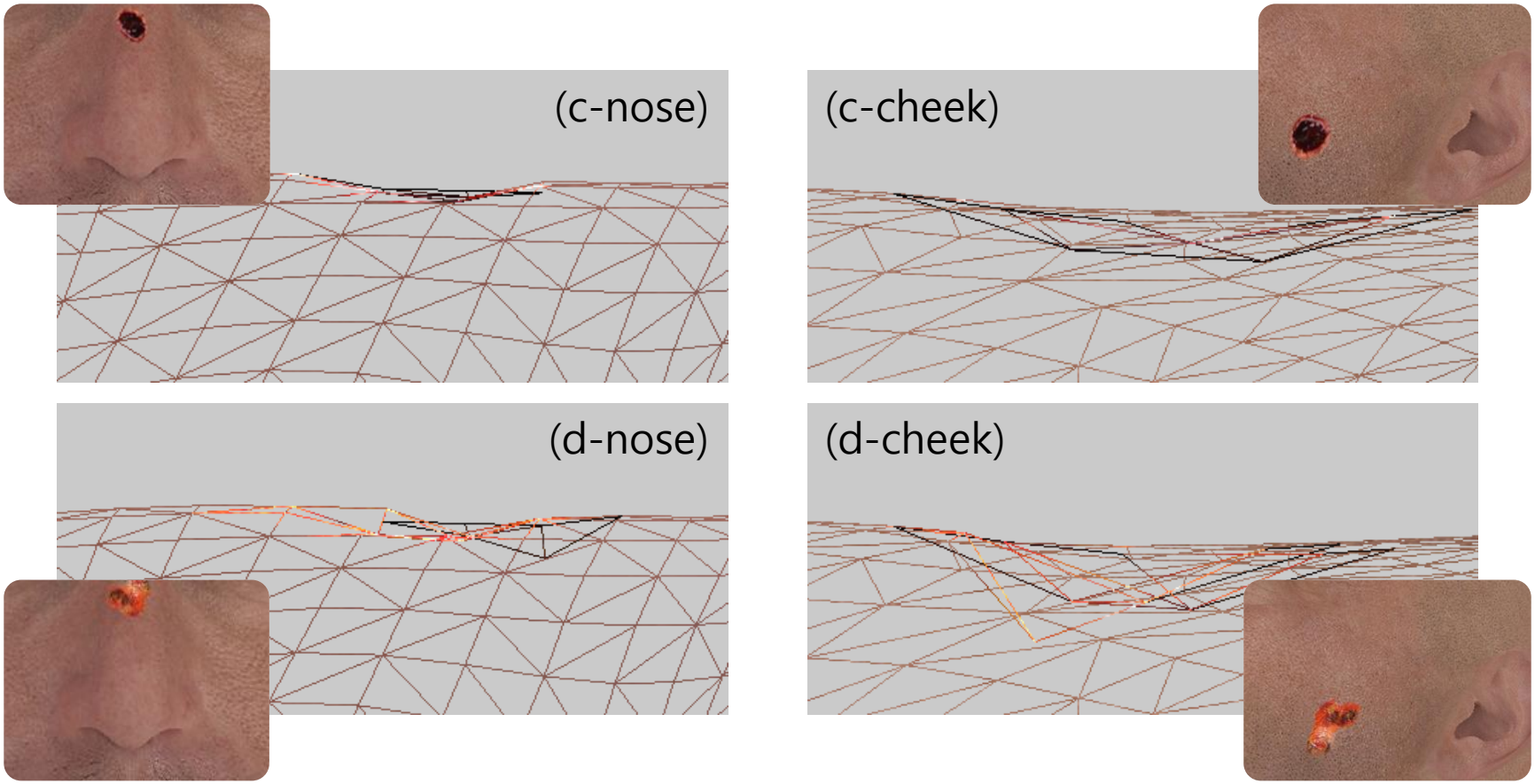

Experimental Results

- Validation of different locations of the face

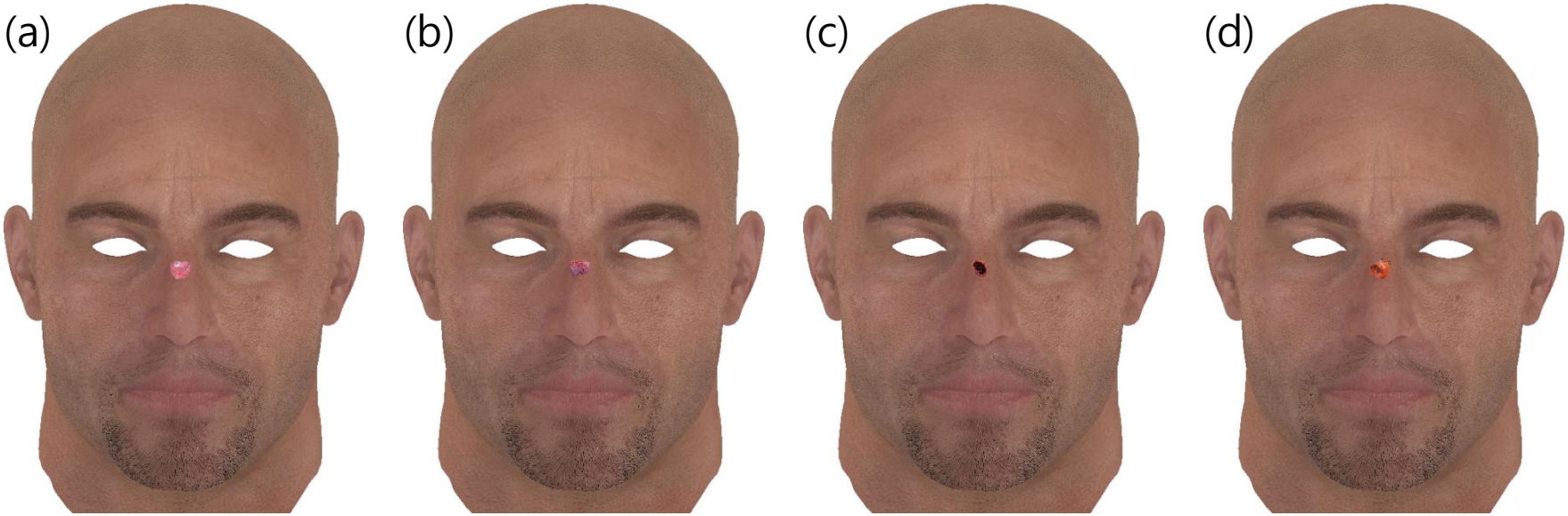

Experimental Results

- Validation of different locations of the face

(a) (b) (c) (d)

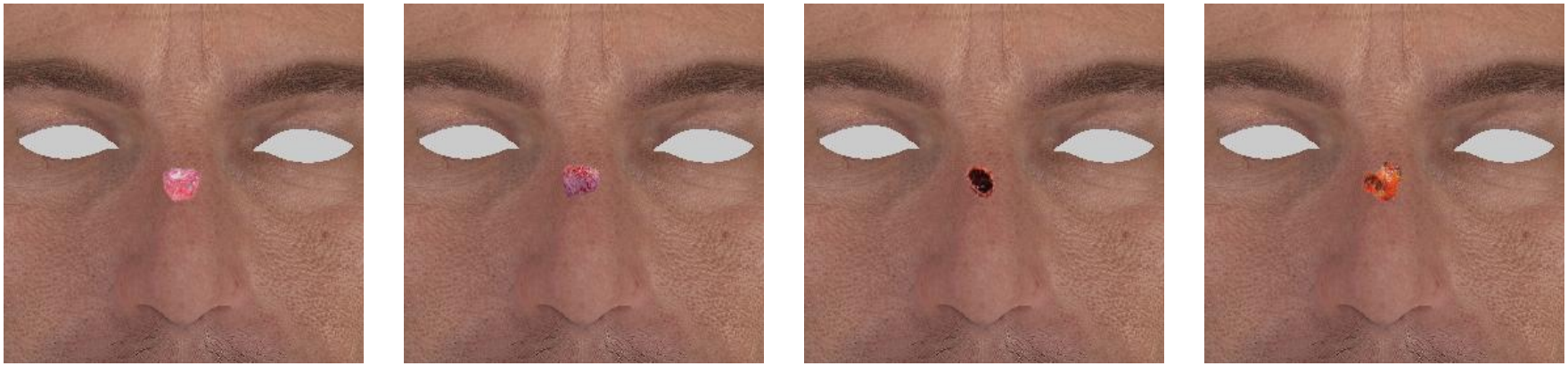

Experimental Results

- Validation of different locations of the face

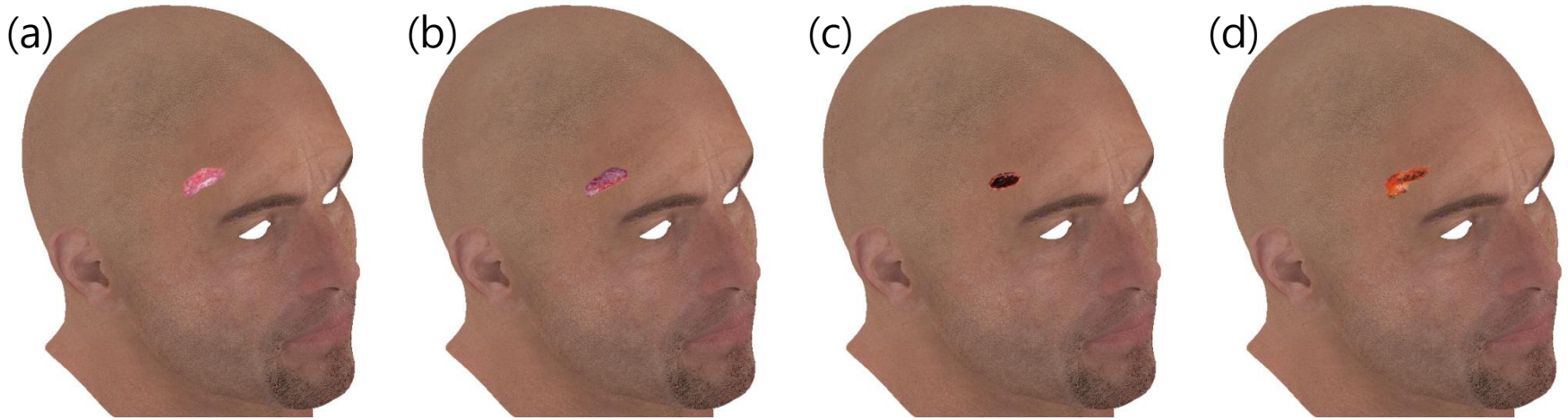

Experimental Results

- Validation of different locations of the face

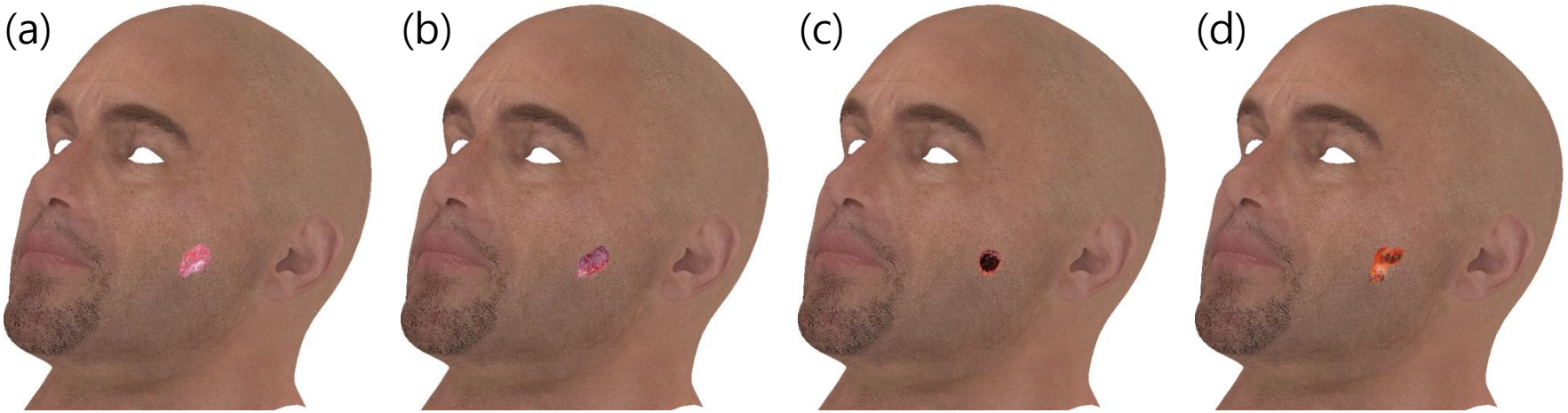

Conclusion

- Summary
  - A multi-layer structural wound synthesis on a 3D face is presented in this research.
  - Using the fact that anatomical skin consists of the epidermis, dermis, and subcutis, we defined a facial depth map, first taking into account various locations on the face.
  - It is possible to segment each skin layer, given an input wound image, using hue values to measure the accurate depth of the wound.
  - In addition, the disparity-based 3D geometry reconstruction is designed to make wound volumetric.
  - To simulate wound synthesis on the face model, we developed a 3d facial wound synthesis system using OpenGL and MFC.
  - It can be used in the fields of virtual surgery, medical training, forensic reconstruction, and archeology as a simple method to attach various types of wounds on 3d virtual face.

Conclusion

- Future works
  - Tissue layer segmentation has been based on hue values after analysing many wound image samples to determine boundary values.
  - However, it would be helpful to have more intelligent decisions regarding the filling of boundary gaps.
  - The synthesised skin tissue needs to be developed in the future, meaning that the epidermis, dermis, and subcutis can be implemented as well, without referring to input wound images.
  - Furthermore, we could extend our approach taking into consideration facial tension line, the degree of transparency of tissue layers, and the variation of wounds corresponding phases of healing as future work

References

- M. Zhang, L. Ma, X. Zeng, and Y. Wang. Image Based 3D Face Modeling. *Proceedings of the Internation al Conference on Computer Graphics, Imaging and Visualization*, 165-168, 2004
- Z. Zhang, Z. Liu, D. Adler, M. Cohen, E Hanson, and Y. Shan. Robust and Rapid Generation of Animated Faces from Video Images: A Model Based Modeling Approach. *International Journal of Computer Vision*, 58(2):93-119, 2004
- A. Hung, K. Mithraratne, M. Sagar, and P. Hunter. Multilayer Soft Tissue Continuum Model: Towards Rea listic Simulation of Facial Expressions. *Proceedings World Academy of Science, Engineering and Technol ogy (WASET)*, 54:134-138, 2009
- Y. Zhang, T. Sim, C.L. Tan, and E. Sung. Anatomy-based face reconstruction for animation using multi-lay er deformation. *Journal of Visual Languages and Computing*, 17:126-160, 2006
- D. M. Cooper. Clinical Assessment/ Measurement of Healing: Evolution and Status. *Clinical Materials*, 8: 263-271, 1991
- C. Glannou and M. Baldan, War Surgery. ICRC. Geneva Switzerland. 2010
- J. Berkley et al. Real-Time Finite Element Modeling for Surgery Simulation: An Application to Virtual Sut uring. *IEEE Transactions on Visualization and Computer Graphics*, 10(3):314-325, 2004

References

- Y. Shen, J. Seevinck, E. Baydogan, Realistic Irrigation Visualization in a Surgical Wound Debridement Si mulator. *Studies in Health Technology and Informatics*, 119:512-514, 2006
- J. Seevinck et al. A Simulation Based Training System for Surgical Wound Debridement. *Studies in Health Technology and Informatics*, 119:491-496, 2006
- C. N. Stephan and E. K. Simpson. Facial soft tissue depths in craniofacial identification (part I): An analyti cal review of the published adult data. *Journal of Forensic Sciences*, 53(6):1257-72, 2008
- F. L. Bookstein. Principal Warps: Thin Plate Splines and the Decomposition of Deformations. *IEEE Trans. Pattern Anal. Mach. Intell.* 11, pp. 567-585, 1989
- T. Igarashi, K. Nishino and S.K. Nayar. The Appearance of Human Skin: A Survey. *Foundations and Tren ds® in Computer Graphics and Vision*, 3(1):1-95, 2007
- F. Veredas, H. Mesa, and L. Morente. Binary Tissue Classification on Wound Images with Neural Network s and Bayesian Classifiers. *IEEE Transactions on Medical Imaging*, 29(2):410-427, 2010
- *http://www.dofmaster.com* (accessed on July 2010)
- C.-Y. Lee and S. Chin. Interactive Wound Synthesis on 3D Face using Inverse Projection Mapping. *Procee dings of the International Congress on Computer Applications and Computational Science (CACS)*, 2010

Thank-you!

This work was partially supported by
National Research Foundation (NRF) grant
funded by the Korea government
(No. 2010-0008673)